Global NEST Journal, Vol 24, No 2, pp 344-349

Adsorption of Cr(VI) on Montmorillonite modified by starch and lanthanum

Su K.*, Deng S.Q., Wang Q., Li L.X., and Cao R.
Faculty of Geosciences and Environmental Engineering, Southwest Jiaotong University, Chengdu 611756, China
Received: 03/03/2022, Accepted: 16/04/2022, Available online: 21/04/2022
*to whom all correspondence should be addressed: e-mail: ksu@swjtu.edu.cn
https://doi.org/10.30955/gnj.004295

Graphical abstract

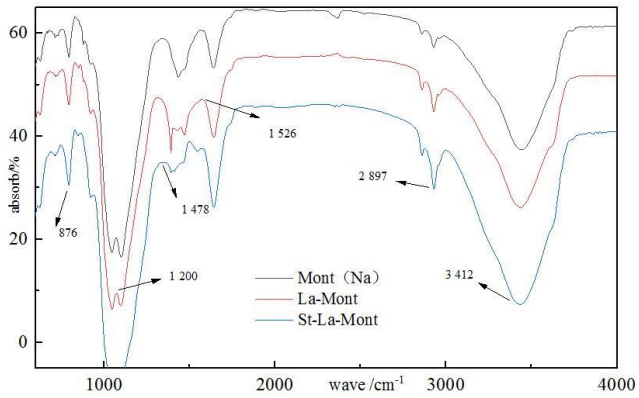

Abstract

Industrial production brings serious Cr(VI) pollution problems, so as to explore new treatment methods for Cr(VI), In this paper, modified montmorillonite was prepared by modifying montmorillonite with starch and lanthanum nitrate, and its adsorption mechanism and effect on Cr(VI) were explored. The modified mechanism and modified monundonerization properties were characterized by Zeta potential, X-ray diffraction (XRD), Fourier Transform infrared spectroscopy (FTIR), and scanning electron microscopy analysis (SEM). The results showed that: Lanthanum-modified montmorillonite and starch-modified lanthanum-modified montmorillonite have better adsorption effects on 10 mg/L Cr(VI) polluted solution, which are 73.9% and 58.6%, respectively, while Na-based montmorillonite Cr(VI) has no adsorption capacity. Both lanthanum and starch only exist on the surface of montmorillonite, which can reduce the overall electronegativity of montmorillonite, so that montmorillonite has the ability to adsorb Cr(VI), at the same time, after the surface of montmorillonite modified by lanthanum nitrate is covered with hydroxyl groups, it is easy to form surface coordination complexes with anions, which further enhances its adsorption effect, and provides a new research idea and direction for the adsorption and removal of Cr(VI).

Keywords: Montmorillonite; Starch; Lanthanum; Cr(VI).

1. Introduction

With the continuous development of the human light industry, the chromium-related chemicals are widely used in industrial production such as ignition, electroplating, thereby producing a problem of chromium wastewater. Chromium mostly exists in the form of trivalent chromium [Cr(III)] and sexivalent chromium [Cr(VI)] in aqueous solution. Some studies have found that the toxicity of the latter is much higher than that of the former, and Cr(VI) has It has stronger migration ability and is easy to bio-accumulate, thereby causing human carcinogenic and mutagenic through the food chain (Katlego *et al.*, 2014). Chinese "Comprehensive Wastewater Discharge Standard"clearly stipulates that the total chromium and Cr(VI) content of chromium-containing wastewater discharged by enterprises should be lower than 1.0 mg/L and 0.2 mg/L. With high concentration, the effect in actual industrial treatment is often unsatisfactory in terms of removal effect or economic cost (Jie Tang *et al.*, 2019). Therefore, the development of an efficient and economical Cr(VI) water removal method has become one of the important topics in the field of water pollution in china.

At present, the treatment methods of chromium-containing wastewater mainly include chemical precipitation, ion exchange, electrolysis and adsorption. The chemical precipitation method will use a large amount of reducing agent and cause secondary pollution problems such as chemical sludge at the same time (Wan Jiang *et al.*, 2021); The ion exchange method has a high technical management threshold in the actual treatment, and there is a risk of being oxidized and causing adsorption failure (Zah A *et al.*, 2021); The electrolysis method cannot be used in actual wastewater treatment on a large scale, and the equipment and consumption are too expensive (Liming Ren *et al.*, 2018); The adsorption method of separating and removing pollutants in sewage through porous adsorbents has gradually become an excellent choice in Cr(VI) wastewater treatment processes due to its advantages of low cost, simple operation, and easy management.

Beverly S developed an activated carbon adsorption model based on artificial neural network, which can effectively predict the removal effect of activated carbon on Cr(VI) (Beverly S *et al.*, 2019); Şeyma Yüksel used almond shells and walnuts to prepare activated carbon, and under optimum conditions, the adsorption capacity of chromium reached 6.67 mg/g (Şeyma Yüksel *et al.*, 2019); Panya Maneechakr explored the preparation of activated carbon from four-cornered windmill as raw material to remove $4mg^{-1}$ of Cr(VI) polluted solution, and finally obtained an adsorption capacity of 1.32 mg/g, which proved that the adsorption method can effectively remove $Cr_2O_7^{2-}$ in the liquid. Although activated carbon as an adsorbent has a good adsorption effect on Cr(VI) and other heavy metals, it is not suitable for large-scale promotion due to its non-renewability and high cost (Panya Maneechakr *et al.*, 2017). As montmorillonite, which can be seen everywhere in nature and is easy to obtain, it also has a stable structure and a large specific surface area, and is widely used as an adsorbent for the adsorption of Cr(VI). Anthony improved the processing efficiency of Cr(VI) to 100% by thermal synthesis of cerium/montmorillonite (Anthony Eric T *et al.*, 2020). Li T achieved an adsorption effect of 156.25 mg/g on Cr(VI) through montmorillonite-supported carbon nanospheres (Li T *et al.*, 2014). Yang Jing modified montmorillonite with tea polyphenols to improve the regeneration activity of Fe, so as to fix Cr(VI) in the soil more friendly(Yang Jing *et al.*, 2021). Zhang Dading prepared a new montmorillonite material loaded with carboxymethyl cellulose, and the adsorption rate of Cr(VI) was increased to 424.6 mg/kg(Zhang Dading *et al.*, 2021). Shengrong Liu used CPC to modify montmorillonite, which reduced the interlayer distance between CPC and montmorillonite and improved the adsorption rate of Cr(VI).(Shengrong Liu *et al.*, 2020).

On the basis of the research on the adsorption of Cr(VI) by montmorillonite, some researchers use specific substances to modify and replace the low-valent cations in montmorillonite to achieve the effect of changing the properties and electrical properties of montmorillonite itself. A montmorillonite modified system was constructed to obtain better adsorption effect. Mirle Vinuth used Fe(II) modification to enhance the adsorption of Cr(VI) in Fe(II)-Mt system under acidic conditions (Mirle Vinuth *et al.*, 2019); B.S. Krishna used polymer materials to improve the positive charge of montmorillonite to improve its adsorption effect. Montmorillonite is electronegative as a whole, and Cr(VI) often exists in the form of dichromate ions in water. Starch is a natural polymer material, and it is electropositive (B.S. Krishna *et al.*, 2000). It has a wide range of sources and is inexpensive. It is possible to coexist with clay minerals such as montmorillonite in nature. Lanthanum (La), as a light rare earth material, can replace low-valent cations in the montmorillonite system, thereby improving its electrical properties. Can a coexisting system of two modifiers and montmorillonite produce a modified material? What is the adsorption effect of the composite modified material shared by two single modified materials and two adsorbents? In this study, montmorillonite was modified individually and in combination with starch and lanthanum nitrate, and the physical and chemical characterization of the modified materials was carried out to explore the adsorption performance of Cr(VI) in aqueous solution, and to reveal the relationship between montmorillonite and natural montmorillonite. The interaction between organic polymers and light rare earth materials, and their possible environmental governance effects, also provide new research ideas and directions for the adsorption and removal of Cr(VI).

2. Materials and methods

2.1. Reagents and instruments

Electronic balance, UV-VIS spectrophotometer, magnetic stirrer (78-1), pH acidity meter (Raymag PHS-3E), water bath constant temperature oscillator (SHZ-82A), desktop low-speed centrifuge (TDA-5A), Electric heating blast drying oven, X-ray diffractometer (Empyrean), Fourier transform infrared spectrometer, high sensitivity Zeta potential and particle size analyzer (nano ZS), field emission scanning electron microscope (SEM).

Montmorillonite (purity>97%), produced in Shijiazhuang City, Hebei Province, its main phase is calcium-based montmorillonite, contains a small amount of quartz impurities, and its chemical components are mainly Si, O, Al, Ca, etc., hardness is 1, the density is about 2 $g.cm^{-3}$, and the purity is 97%; Acetic acid, experimental corn starch, sodium hydroxide, sodium chloride, potassium dichromate, all purchased from Shanghai Aladdin Biochemical Technology Co., Ltd.; concentrated Sulfuric acid and concentrated nitric acid were purchased from Shanghai Standard Technology Co., Ltd. All the above reagents except montmorillonite are of analytical grade. The test water was deionized water.

2.2. Sample preparation

2.2.1. Preparation of Na-based montmorillonite (Na-Mont)

Dissolve 10 g of 97% high-purity montmorillonite [Montmorillonite (hereinafter referred to as Mont)] and 1 mol/L NaCl in a 250 mL volumetric flask, stir in a magnetic stirrer for 24 h, remove the supernatant by centrifugation and deionize washed with water, dried in an electric blast drying oven at 65° C. for 24 hours, and crushed to obtain Na-based montmorillonite (Na-Mont).

2.2.2. Preparation of La-Modified Montmorillonite (La-Mont)

Weigh 4g of lanthanum nitrate hexahydrate $[La(NO)_3]_3{\cdot}6H_2O$ and 10g of prepared Na-Mont to dissolve in a 250 mL volumetric flask, stir in a magnetic stirrer for 8h, and remove the supernatant by centrifugation and washed with deionized water, dried in an electric heating blast drying oven at 65° C. for 24 hours, and crushed to obtain Na-based montmorillonite (La-Mont).

2.2.3. Preparation of Starch Modified La Montmorillonite (St-La-Mont)

Weigh 1 g of test starch (St), dissolve it in 50 mL of acetic acid (5%), add 10 g of the prepared La-Mont, stir in a magnetic stirrer for 24 h, remove the supernatant by

centrifugation and wash with deionized water, dried in a high-temperature drying oven at 65°C for 24 hours, and crushed to obtain a starch-modified montmorillonite (St-La-Mont).

2.3. Test process

Weigh an appropriate amount of $K_2Cr_2O_7$ and dissolve it in a 1 L volumetric flask to prepare a solution with a concentration of 30 mg/L $K_2Cr_2O_7$ for use. The contaminated solution was shaken in a water bath thermostatic oscillator at 30°C for 8 hours (200 r/min), centrifuged and the supernatant was taken. The concentration of Cr(VI) was measured by UV-Vis spectrophotometer, and Cr was obtained according to formula (1). (VI) removal rate. Three groups of parallel samples were set up in the experiment and the average value was taken. The removal rate of Cr(VI) is shown in the following formula.

$$\eta = \left(\frac{Co - Ce}{Co} \right) \quad (1)$$

In the formula: initial concentration of Co—Cr(VI), mg/L; Ce—concentration of Cr(VI) in solution after the adsorption reaches equilibrium, mg/L; η—Cr(VI) adsorption rate.

2.4. Sample Characterization

The spatial structure of the material was characterized by X-ray diffractometer (XRD), and the state between the material layers was analyzed. Fourier transform infrared spectroscopy (FTIR) was used to characterize the types of surface functional groups and chemical bonds. Zeta potential was characterized by high-sensitivity Zeta potential and particle size analyzer (nano ZS), and the amount of charges on the surface before and after montmorillonite modification was analyzed. The morphology of montmorillonite before and after modification was observed by field emission scanning electron microscope (SEM).

3. Results and discussion

3.1. X-ray diffraction characterization

The X-ray diffraction characterization of Mont, La-Mont and St-La-Mont is carried out, and the results are shown in Figure 1. According to the diffraction patterns, it can be seen that Mont and La-Mont have almost the same diffraction peaks around 25~30°, indicating that the two have a certain similarity in surface structure. The modification of La did not bring a new structure to the surface of the Mont crystal, and there was no obvious numerical difference in the diffraction 2θ angles of the three, indicating that La-modified Mont and St-modified La-Mont both changed the interlayer domain of the two. Mont and La-Mont have the same diffraction peak at 29.36° (Wang Xin *et al.*, 2021), but St-La-Mont has no diffraction peak at this position, indicating that the modification of La-Mont by St changes Mont and La-Mont through surface wrapping. The diffraction peaks shift to high angles, indicating that St modification reduces the interlayer spacing of montmorillonite and reduces the thickness of the interlayer domain of Mont. It is speculated that it may be because St does not enter the interlayer domain of Mont, but wraps it outside it. the diffraction peak at 29.36° has a certain influence on the adsorption efficiency of Cr(VI). At the same time, according to the literature review, the loading of La in this study is not large, and it is difficult to capture the diffraction peaks of lanthanum at a scanning speed of 10°/min by XRD (Frois S R *et al.*, 2012).

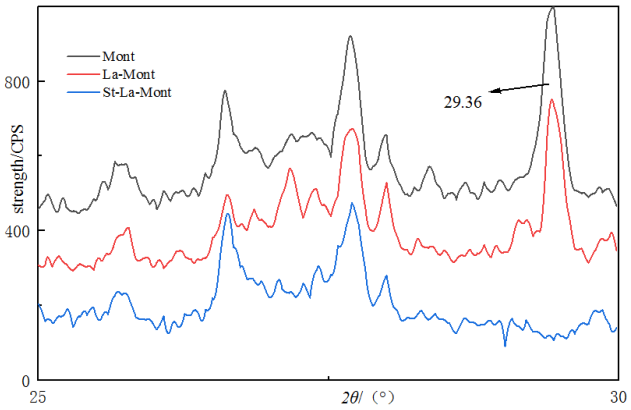

Figure 1. XRD Phenogram.

3.2. Fourier transform infrared spectroscopy FTIR characterization

In order to determine whether there are chemical changes between montmorillonite and starch during the modification process and whether the modification affects the surface functional groups of montmorillonite, Mont, La-Mont and St-La-Mont were characterized by FTIR, respectively as shown in picture 2, When the peak positions are 3412 cm^{-1} and 1478 cm^{-1}, peaks appear in the Mont, La-Mont and St-La-Mont curves. In contrast, the peak of St-La-Mont is weakened, which may be caused by the stretching vibration of water molecules between La-Mont and St interlayers (O-H). At the same time, it can be seen that La-Mont has obvious vibration enhancement in the peak area at 1478 cm^{-1} compared with Mont, which indicates that La reacts to Mont mainly with O-H (Larraza I *et al.*, 2012). When the wave number is 2897 cm^{-1}, the three peaks also appear, which is due to the fact that both Mont and La-Mont contain a large number of CH_2 structures, which are caused by the C-H symmetrical stretching vibration between the CH_2 structures; When the peak position is 1526 cm^{-1}, peaks appear in the curves of Mont, La-Mont and St-La-Mont, which are caused by the C-O stretching vibration. When the peak position is 876 cm^{-1} and 1200 cm^{-1}, the common curves of Mont, La-Mont and St-La-Mont appear, which may be due to the fact that the three are modified based on Mont, so that their substances contain Si(Al)-O stretching vibration.

At the same time, it can be seen from the FTIR scan pictures of the three that there is not much difference in the infrared spectra of the three on the wave crest. The front and rear migrations are all within the error range, and no new characteristic spectrum is formed. If La enters the internal structure of Mont and participates in the skeleton vibration, the Si-O bond bending vibration of the

modified La-Mont will become larger and the wave number will decrease. It can be seen from the figure that such a situation does not occur, indicating that the reaction with Cr(VI) is mainly due to the electrostatic adsorption between La on the surface of Mont (Figure 2; Yang-Min *et al.*, 2018).

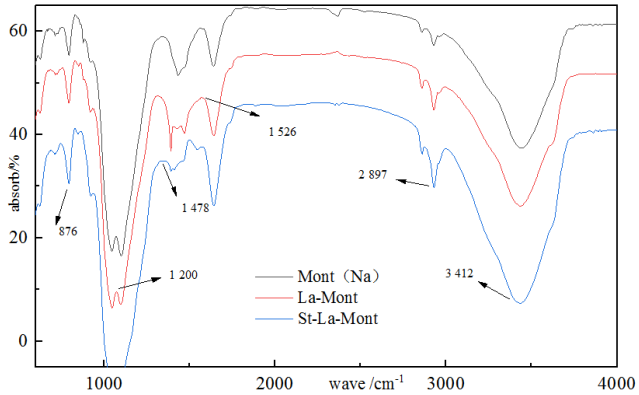

Figure 2. FTIR spectra diagram of Mont, La-Mont, St-La-Mont.

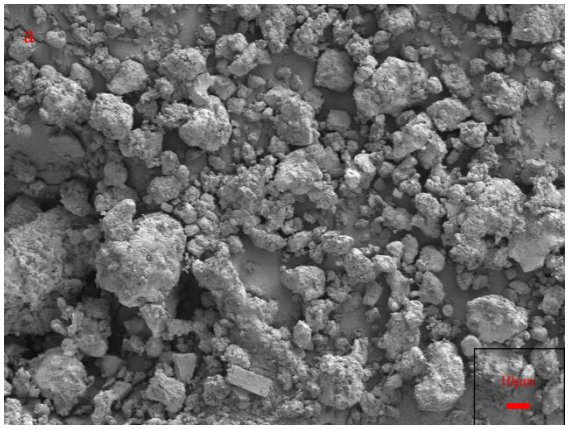

Figure 3. Structural equation modeling spectra diagram of Na-Mont(a).

3.3. Scanning electron microscope (SEM) characterization

Through further scanning electron microscope image analysis of Mont, La-Mont and St-La-Mont, the combination of La and St with La-Mont was explored. It can be seen from the figure that the surface stacking phenomenon of the three shows the stacking difference of St-La-Mont, La-Mont and Mont from dense to scattered, It can be clearly seen that the particle size of Figure 3 is smaller and the arrangement is neat and orderly, while the particle size of Figures 4 and 5 is significantly larger and denser, which indicates that La-Mont and St-La-Mont Some particles on the surface have agglomeration effect, and a certain degree of agglomeration occurs. La-Mont and St-La-Mont have obvious lateral synaptic structure compared with Mont, and the structure similar to lateral synapse with surrounding fine particles is La element (Sahu Sumanta *et al.*, 2021). At the same time, it can be seen that after St modification of La-Mont, the La element distributed on the surface is obviously reduced, and replaced by uniformly distributed St particles. The FTIR scanning results show that La entering the surface of Mont is mainly loaded on its surface, During the modification process of La and Mont, the solution of Mont gradually formed metal oxides and hydroxides, and on the surface of these metal oxides, due to the coordinative unsaturation of its surface ions, it coordinates with water in an aqueous solution to form a hydroxylated surface. The surface hydroxyl groups can undergo proton migration in solution, showing amphoteric surface characteristics and corresponding charges. The modified Mont surface After covering the hydroxyl groups, it is easy to form surface coordination complexes with anions (You-Wei *et al.*, 2017), which is also the reason why La modification greatly improves the adsorption effect of Cr(VI).

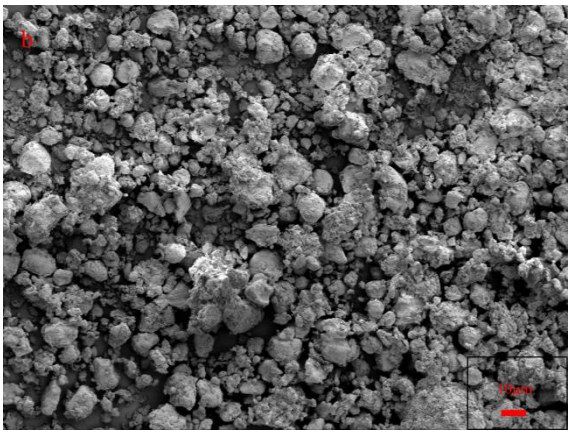

Figure 4. Structural equation modeling spectra diagram of La-Mont(b).

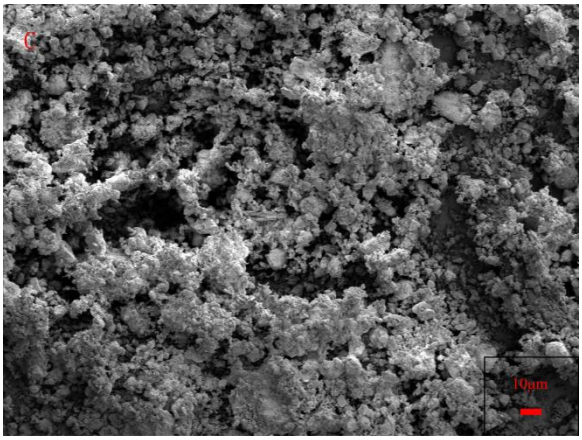

Figure 5. Structural equation modeling spectra diagram of St-La-Mont(c).

3.4. Zeta potential characterization

In order to determine the change of the overall electrical properties of La and St before and after the modification process, the Zeta potential characterization of Mont, La-Mont and St-La-Mont was carried out respectively. As shown in Figure 6, the potential of Na-Mont is -21.2mV , the La-Mont potential is -12.7mV, and the St-La-Mon potential is -10.9mV. La and St are both positively charged, so the modification effectively increases the potential of Na-Mont and La-Mont, that is, reduces their overall electronegativity. It is worth noting that the mass ratio of St-modified Na-Mont in this paper is 1:10, which fails to change Na-Mont to electropositivity.

3.5. Adsorption of Cr(VI) by Na-Mont, St, St-Mont

Experiments were carried out according to the experimental procedure of 1.3, and finally the adsorption results of Mont, La-Mont and St-La-Mont on 10 mg/L Cr(VI) were obtained, as shown in Figure 7. The research results show that Na-Mont has almost no adsorption effect on Cr(VI), La-Mont and St-La-Mont have good adsorption effect on Cr(VI)(between 50% and 75%). It can be seen from the FTIR analysis that Mont, La-Mont and St-La-Mont have similar peak positions in the 0-4000 cm^{-1} peak position. But Sem analysis shows that La-modified Mont surface is covered with hydroxyl groups, and it is easy to form surface coordination complexes with anions, which can be removed by reacting with negatively charged $Cr_2O_7^{2-}$ in solution (Jianjun Yuan *et al.*, 2014). It is also because the modification of La and Mont only stays on the surface of Mont, so after St loading La-Mont, St particles wrap the shell of La-Mont, which reduces the chance of direct contact with $Cr_2O_7^{2-}$, so although St is further reduced the electrical properties of La-Mont, However, it reduces the effect of complex adsorption between La-Mont and $Cr_2O_7^{2-}$, so its adsorption effect is 58.6% less than that of La-Mont, which is 73.9%, but it also reduces the negative charge of Mont, so its adsorption effect is higher than that of Mont 1.5%.

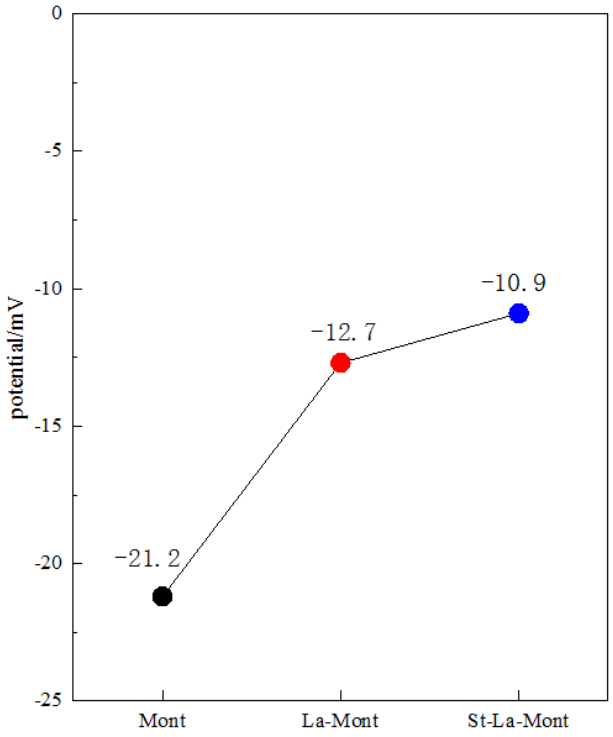

Figure 6. The Zeta potential of Mont, La-Mont, St-La-Mont.

Combined with the Zeta potential characterization results of Mont, La-Mont and St-La-Mont on Cr(VI), it can be seen that Mont is electronegativity as a whole, while Cr(VI) exists in the form of $Cr_2O_7^{2-}$ ions in aqueous solution, and is in the Coulomb repulsion force. Under the action of, there is almost no adsorption reaction between Mont and Cr(VI). The electronegativity of La-Mont is reduced due to the modification of La, so that its adsorption capacity for Cr(VI) has been significantly improved. At the same time, since the surface of La-modified La-modified Mont is covered with hydroxyl groups, it is easy to form with anions. Surface coordination complex, the removal rate reached 73.9%. At the same time, according to FTIR and SEM analysis, St stays on the surface of La-Mont and has surface stacking phenomenon, which further reduces the negative charge of St-La-Mont and increases its adsorption rate to 58.6%. The encapsulation effect masks the original diffraction peak of La-Mont at 29.36°, which reduces the effect of La modification, and the overall adsorption efficiency is also lower than 73.9% of La-Mont.

4. Conclusion

La-Mont and St-La-Mont composites were prepared in this study. La and St modification may only exist on the surface of montmorillonite, which reduces the overall electronegativity of Mont. The change of the overall electrical properties of St-Mont makes St-Mont have the ability to adsorb Cr(VI). At the same time, after the surface of La-modified Mont is covered with hydroxyl groups, it is easy to form surface coordination complexes with anions, which further enhances its adsorption effect.

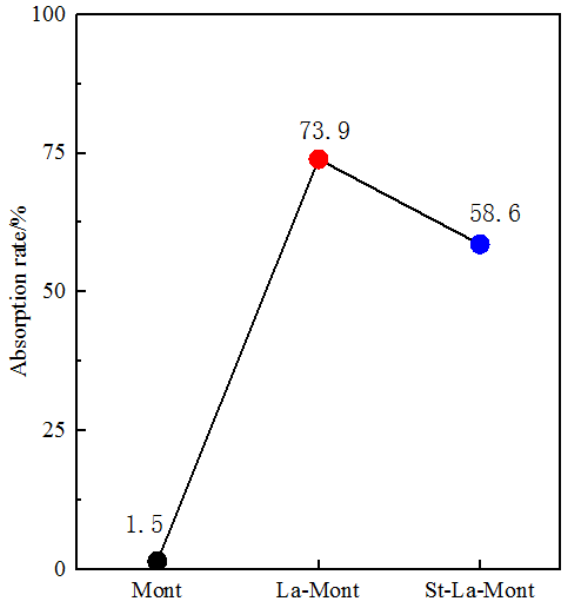

Figure 7. Chromium(VI) adsorption effect of Mont、La-Mont、St-La-Mont.

In this study, environmentally friendly and inexpensive montmorillonite and starch, which are ubiquitous in nature, were selected as the base material and modifier, respectively, to study the adsorption effect of Cr(VI) ions in water. The modification and its adsorption of heavy metals have theoretical significance, which provides a new research idea and direction for the adsorption and removal of Cr(VI) ions.

Acknowledgement

This work was supported by Sichuan Science and Technology Program (2021YFS0284), the Opening Project of Key Laboratory of Theoretical Chemistry of Environment (South China Normal University), Ministry of Education (20200103), the Fundamental Research Funds for the Central Universities of Southwest Jiaotong University (210824), and the Opening Project of Key Laboratory of Southwest Jiaotong University (ZD2021210001).

References

Chittoo B.S., Venkobachar C., and Sutherland C. (2019). Application of ANN predictive model for the design of batch adsorbers - equilibrium simulation of Cr(VI) Adsorption onto Activated Carbon. *The Open Civil Engineering Journal*, **13**, 1107–1119.

Cui Y-W., Jie L., ZhaoFu D., and YongZhen P. (2018). Cr(VI) adsorption on red mud modified by lanthanum: performance, kinetics and mechanisms. *PLoS ONE*, **11**, 1205–1218.

Eric A., Moses A., and Toyin S. (2020). One-pot thermal synthesis of Ceria/Montmorillonite composite for the removal of sexivalent chromium from aqueous system. *Surfaces and Interfaces*, **22**, 232–247.

Frois S.R., Grassi M.T., and Campos M.S.D. (2012). Determination of Cr(VI) in water samples by ICP-OES after separation of Cr(III) by montmorillonite. *Analytical Methods*, 73–89.

Jie T., Bin M., and Zong L. (2019). From waste hot-pot oil as carbon precursor to development of recyclable attapulgite/carbon composites for wastewater treatment. *Journal of Environmental Sciences*, **75**, 346–358.

Jing Y., Wang S.Q., Nan X., Zhi Y., Han Y., and Xinxing H. (2021). Synthesis of montmorillonite-supported nano-zero-valent iron via green tea extract: Enhanced transport and application for hexavalent chromium removal from water and soil. *Journal of Hazardous Materials*, **419**, 12–17.

Krishna B.S., Murty D.S.R., and Prakash J. (2000). Thermodynamics of chromium(VI) anionic species sorption onto surfactant-modified montmorillonite clay. *Journal of Colloid And Interface Science*, **229**, 112–126.

Larraza I., López M., and Corrales T. (2012). Hybrid materials: Magnetite Polyethylenimine Montmorillonite, as magnetic adsorbents for Cr(VI). *Water Treatment. J Colloid Interface*, **385**, 50–56.

Li T., Shen J., and Huang S. (2014). Hydrothermal carbonization synthesis of a novel montmorillonite supported carbon nanosphere adsorbent for removal of Cr (VI) from waste water. *Applied Clay Science*, 2014, **93–94**, 48–55.

Liu S.R., Ming C., Cao X.Q.., Guang L., Di Z., Li M.Z., Meng N., Yin J.J., and Yan B.Q. (2020). Chromium (VI) removal from water using cetylpyridinium chloride (CPC)-modified montmorillonite. *Separation and Purification Technology*, **241**, 435–452.

Ma Y.M., Tong L., and Huang W.H. (2018). Synthesis of a 3D lanthanum(III) MOFs as a multi-chemosensor to Cr(VI) containing anion and Fe(III) cation based on a flexible ligand. *Journal of Solid State Chemistry*, **258**, 476–481.

Maneechakr P.Y., and Karnjanakom S.C. (2017). Adsorption behaviour of Fe(II) and Cr(VI) on activated carbon: Surface chemistry, isotherm, kinetic and thermodynamic studies. *The Journal of Chemical Thermodynamics*, **106**, 73–75.

Ren L.M., Jung D., Chi Z.F., and Huang H.Z. (2018). Reduced graphene oxide-nano zero value iron(rGO-nZVI) micro-electrolysis accelerating Cr(VI) removal in aquifer. *Journal of Environmental Sciences*, **73**, 6–106.

Sahu S., Nisarani B., Sahu K., and Patelraj K. (2021). Investigating the selectivity and interference behavior for detoxification of Cr(VI) using lanthanum phosphate polyaniline nanocomposite via adsorption-reduction mechanism. *Chemosphere*, **278**, 109–118.

Setshedi K.Z., Bhaumik M., Onyango M.S., and Arjun M. (2014). Breakthrough studies for Cr(VI) sorption from aqueous solution using exfoliated polypyrrole-organically modified montmorillonite clay nanocomposite. *Journal of Industrial and Engineering Chemistry*, **20**, 64–67.

Şeyma Y., and Orhan R. (2019). The removal of Cr(VI) from aqueous solution by activated carbon prepared from apricot, peach stone and almond shell mixture in a fixed-bed column. *Arabian Journal for Science and Engineering*, **44,** 52–54.

Vinuth M., Naik M., Karthik H.S., and Bhojya Naik K. H. (2019). Hemakumar. Detailed study on reduction of hazardous Cr(VI) at acidic pH using modified montmorillonite Fe(II)-Mt under ambient conditions. *Research on Chemical Intermediates*, **45,** 109–118.

Wang X.J., Wei Y., and Hui L. (2021). Strength and microstructural analysis of geopolymer prepared with recycled geopolymer powder. *Journal of Wuhan University of Technology(Materials Science)*, **36**, 39–445.

Yuan J.J., Yin H.C., Bo J., Zheng J.T., Zhu C.S., Sun G.H., Qiu S., Han W., Yang L., Jingwei Z., Mingbo W., Wenting W., and Huijiao X. (2014) Simultaneous Photocatalytic Reduction and Removal of Cr(VI) on TiO2 Immobilized by ACF. *Journal of Advanced Oxidation Technologies*, **17**, 56–63.

Zah A., Ira A., and Nha B. (2021). Liquid ion exchange methodology for extraction Cr (VI) using azo derivative compound. *Materials Today: Proceedings*, 34–43.

Zhang D.D., Xu Y.Q., Li X.F., Liu Z.H., Wang L.N., Lu C.J, He X.W., Yan M., and Zou D.X. (2020). Immobilization of Cr(VI) in soil using a montmorillonite-supported carboxymethyl cellulose-stabilized iron sulfide composite: effectiveness and biotoxicity assessment. *International Journal of Environmental Research and Public Health*, **17**(17), 17–19.